



## Investigation of Photocatalytic Removal and Photonic Efficiency of Maxilon Blue Dye GRL in the Presence of TiO<sub>2</sub> Nanoparticles

Enas M. Alrobayi, Abrar M. Algubili, Aseel M. Aljeboree, Ayad F. Alkaim & Falah H. Hussein

To cite this article: Enas M. Alrobayi, Abrar M. Algubili, Aseel M. Aljeboree, Ayad F. Alkaim & Falah H. Hussein (2015): Investigation of Photocatalytic Removal and Photonic Efficiency of Maxilon Blue Dye GRL in the Presence of TiO<sub>2</sub> Nanoparticles, Particulate Science and Technology, DOI: [10.1080/02726351.2015.1120836](https://doi.org/10.1080/02726351.2015.1120836)

To link to this article: <http://dx.doi.org/10.1080/02726351.2015.1120836>



Accepted author version posted online: 30 Nov 2015.



Submit your article to this journal [↗](#)



View related articles [↗](#)



View Crossmark data [↗](#)

# Investigation of Photocatalytic Removal and Photonic Efficiency of Maxilon Blue Dye GRL in the Presence of TiO<sub>2</sub> Nanoparticles

Enas M. Alrobayi

Department of Laser Physics, College of Sciences for Women, Babylon University, Hilla, Iraq

Abrar M. Algubili

Department of Laser Physics, College of Sciences for Women, Babylon University, Hilla, Iraq

Aseel M. Aljeboree

Department of Chemistry, College of Sciences for Women, Babylon University, Hilla, Iraq

Ayad F. Alkaim\*

Department of Chemistry, College of Sciences for Women, Babylon University, Hilla, Iraq

Falah H. Hussein

College of Pharmacy, Babylon University, Hilla, Iraq

Address correspondence to Ayad F. Alkaim. Tel.: +964 780 132 4986. E-mail: alkaim@iftc.uni-hannover.de

## Abstract

TiO<sub>2</sub> nanoparticles have been synthesized by solvent free-hydrothermal. TiO<sub>2</sub> nanoparticles were annealed at 500°C for enhancing characterization and the photocatalytic activity. The

synthesized TiO<sub>2</sub> was characterized by X-ray diffraction (XRD), field emission scanning electron microscopy (FE-SEM), atomic force microscopy (AFM), BET, and diffuse reflectance spectroscopy (UV-DR) techniques to study the morphology, and structural configuration. The effects of different parameters such as the initial dye concentration, catalyst concentration, pH of the solution, light intensity and reactive oxygen species (ROSs) on relative photonic efficiencies and photocatalytic degradation kinetics of GRL were investigated, the degradation of GRL follows pseudo-first order kinetics according to the Langmuir–Hinshelwood model. The reactive oxygen species studies indicate that hydroxyl radicals and holes are the predominant reactive species within the same step, contributing up to 92.64%, hydroxyl radicals participate for about 55%, and holes share for about 37.64% in the photocatalytic degradation of GRL.

**Keywords:** maxilon blue dye, photocatalytic removal, photonic efficiency, reactive oxygen species, titanium dioxide, UVA-LED

## INTRODUCTION

Undoubtedly, today the environmental pollutants, consider as important problems in the human society. Water pollution requires main solutions because it is one of the most unfavorable environmental problems in the world. Textile industries produce a lot of wastewater, which contains a number of undesirable compounds, including caustic dissolved solids or acidic and poisonous compounds. A lot of organic dyes (synthetic dyes) are hazardous and may do affect water life causing different diseases (Vieira et al. 2009).

There are many ways for pollutant elimination such as adsorption on activated carbon, reverse osmosis, ultra-filtration, and etc.(Tang and An 1995; Simin 2014; Aljeboree, Alkaim, and Al-Dujaili 2015; Fil 2015) these methods generally cause transferring the organic pollutants

from water to other media that naturally produce a new pollution. In recent decades, a growing need for green technology has facilitated the development of alternative technologies that avoid the consumption of excessive chemicals and minimize the generation of toxic sludge after treatment (Zhou and Smith 2002). In this regard, advanced oxidation processes (AOP) such as ozone, Fenton's oxidation, ultrasound, electro-oxidation, and photocatalytic degradation have been identified as one of the most promising options for this purpose through the formation of OH radicals (Wang et al. 2010; Bayar et al. 2014; Fil et al. 2014; Alkaim, Dillert, and Bahnemann 2015; Islam, Kurny, and Gulshan 2015; Kul et al. 2015).

Photocatalytic degradation is an important process for wastewater treatment. In particular, this method is notably useful for purification of wastewater containing organic contaminants (Alkaim and Hussein 2012; Kandiel et al. 2013; Da Dalt et al. 2015; Sobana, Krishnakumar, and Swaminathan 2013). This technique has certain advantages over other processes, such as a small amount of by-products, complete mineralization, cost effectiveness, and applicability at moderate temperatures (Sun et al. 2006; El-Mekkawi and Galal 2013). Among many proposed semiconductors for photocatalytic treatment, titanium dioxide is a suitable photocatalyst because of its acceptable band gap energy, easy availability and low cost (Thiruvengatchari, Vigneswaran, and Moon 2008). Such photocatalysts apply UV light to generate electron-hole pairs at their conduction and valence bands (Gaya and Abdullah 2008). Then the electrons in the conduction band react with molecular oxygen in bulk solution to generate active oxidant species such as superoxide radical anions and hydrogen peroxide. On the other hand, the holes at valence band can oxidize surface hydroxyl groups to form **OH**<sup>•</sup> radicals or even organic pollutant molecules (Kansal et al. 2014). The mentioned oxidant species attack the organic pollutant targets leading to eventually oxidation of them to CO<sub>2</sub>, H<sub>2</sub>O, and etc.

Large amount of dyes are annually used in different kinds of industries such as textile, cosmetics, food, pharmaceutical, and paper industries (Pitchaimuthu et al. 2014). The largest and the most important classes of commercial dyes have been found in azo dyes constitute.

The removal of azo dyes is an important process, because many azo dyes are toxic to aquatic organisms(Chen 2009), therefore in this work we choose a maxilon blue (GRL) as a model of azo-dye pollutant(Aljebori and Alshirifi 2012), and to investigate the photocatalytic degradation of synthesized TiO<sub>2</sub> nanoparticles. The effect of operational parameters such as catalyst concentration, dye initial concentration, UVA light intensity, and pH of the solution on the relative photonic efficiency of synthesis TiO<sub>2</sub> nanopartilces photocatalysis as well as the role of reactive oxygen species (ROSs) on the photo-removal and relative photonic efficiency trends in the photocatalytic degradation of maxilon blue dye GRL have also been investigated.

## **MATERIALS AND METHODS**

### **Materials**

Titanium(IV) bis(ammoniumlactato) dihydroxide (TALH, 50% aqueous solution), aqueous ammonia solution (28.0–30.0% NH<sub>3</sub>), sodium hydroxide (98%), Nitric acid (70%), Ethylenediaminetetraacetic acid disodium salt dehydrate (Sigma-Aldrich), 2-propanol anhydrous, (99.5% Sigma-Aldrich), Potassium iodide anhydrous (99.5%, Sigma-Aldrich), nitric acid (70%, Sigma-Aldrich), N-phenylaniline (Merck Millipore), Maxilon blue dye (GRL) was obtained from Al-Hilla of textile industries/Iraq. All the chemicals were used as received, without further purification.

### **Methods**

Pure anatase TiO<sub>2</sub> nanoparticles with 97 m<sup>2</sup> g<sup>-1</sup> have been synthesis by the thermal hydrolysis of titanium(IV) bis(ammoniumlactato) dihydroxide (TALH) as previously reported with annealing modifications (Alkaim et al. 2013). Typically, 10 mL of an aqueous titanium(IV) bis(ammoniumlactato) dihydroxide solution was mixed with an aqueous ammonia solution. The resulting solution volume was 100 mL and the concentration of aqueous ammonia was adjusted to be 1.0 M was mixed with constant stirring at room temperature. Subsequently, the resultant solution was transferred into a Teflon-lined stainless steel autoclave with a volume of 250 mL. Then, the Teflon cup was sealed in an autoclave and placed into an electric furnace held at 160°C for 24 h.

After the growth, it was allowed to cool down naturally to room temperature; the resulting TiO<sub>2</sub> nanoparticles were collected, washed with water/ethanol different times with ultrasonic assistance, then dried at 80°C for 24 h and finally annealed at 500°C for 4 h. The synthesized sample was characterized by XRD, the Brunauer–Emmett–Teller (BET) surface area; UV–Vis. diffused reflectance spectra (DRS), Field-emission scanning electron microscopy (FE-SEM), and NTMDT Solver (P47-PRO) scanning probe microscope operating in the contact atomic force microscopy (AFM) **mode with a scan speed of 1 Hz.**

The photocatalytic degradation experiments were carried out in a batch photoreactor, reaction suspensions (200 mL) containing a suitable amount of TiO<sub>2</sub> photocatalyst and GRL dye solution were kept in darkness for 60 min, in the presence of oxygen bubbling in order to reach adsorption–desorption equilibrium. The reactor contained a stirring rod supported by a magnetic stirrer to confirm homogeneity of the mixture throughout the reactor; all the experiments were done at room temperature (30°C). The pH of dye solutions was adjusted by adding 0.05 M HNO<sub>3</sub> or NaOH.

The reaction was initiated when LED/UVA (365 nm-Collimated LED for Olympus BX & IX, 700 mA Thorlab/USA) intervals light bulbs (measured by UVA radiometer, Dr Honle/Germany) were switched on. Samples were taken out at specific time intervals and centrifuged at 3500 rpm. The remaining concentration of GRL in solution was analyzed by UV-vis spectrophotometer (UV 1650 spectrometer, Shimadzu) at its maximum wavelength of 609 nm.

An estimate of the contribution of hydroxyl radicals for  $\text{OH}^\cdot$ , oxygen superoxide radical  $\text{O}_2^\cdot$  and positive holes (h+) during the heterogeneous photocatalytic degradation of GRL dye are determined by adding different concentrations of reactive oxygen species ROSs: isopropyl alcohol (IPA), diphenylamine (DPA), Potassium iodide (KI) and Ethylenediaminetetraacetic acid disodium salt dehydrate ( $\text{Na}_2\text{EDTA}$ ) were added in different concentrations (0.005, 0.01, 0.05, and **1 mM**) to the reaction solution.

The relative photonic efficiency, photocatalytic degradation efficiency, apparent first order rate constant of photocatalytic degradation of GRL dye and were calculated using the following relationships

$$\varepsilon = \frac{R \cdot V}{I_0 \cdot A} \quad (1)$$

$$I_0 = \frac{I \cdot \lambda}{N_A \cdot h \cdot c} \quad (2)$$

$$\text{PDE}(\%) = 100 \times (C_0 - C_t) / C_0 \quad (3)$$

$$\ln \frac{C_t}{C_0} = -kt \quad (4)$$

Where,  $R$  is the rate of photocatalytic degradation ( $\text{mg.L}^{-1}.\text{min}^{-1}$ ),  $\epsilon$  is the relative photonic efficiency,  $V$  is volume of irradiated solution (L),  $A$  is the irradiation area of photocatalytic reaction,  $I$  is the incident light of irradiation source ( $\text{mW cm}^{-2}$ ),  $\lambda$  is the wavelength of irradiation source (m),  $N_A$  is the Avogadro's number,  $h$  is the Planck constant,  $c$  is the speed of light in space,  $C_0$  and  $C_t$  are the initial and photolyzed concentration ( $\text{mg L}^{-1}$ ), respectively, PDE(%) is photocatalytic degradation efficiency,  $t$  is time of irradiation (min.) and  $k$  is the apparent first order rate constant ( $\text{min}^{-1}$ ).

## RESULTS AND DISCUSSION

### Characterization of $\text{TiO}_2$ Photocatalysts

The XRD pattern of annealed  $\text{TiO}_2$  is illustrated in **Figure (1a)**. The intensified diffraction peaks of annealed  $\text{TiO}_2$  at  $2\theta = 25.56, 38.02, 48.3, 54.14, 55.27, 62.69, 68.9, 70.52$  and  $75.22$  were assigned to a pure anatase phase (Gnanaprakasam et al. 2015). No Rutil or Brookite peak was observed, clearly depicting that the crystallization of synthesized  $\text{TiO}_2$ . The crystalline size of the annealed  $\text{TiO}_2$  was examined by using Scherrer's equation,  $D = 0.9\lambda/\beta \cos \theta$ , where  $\beta$  is the full width at half maximum intensity,  $\lambda$  is the wavelength of  $\text{Cu-K}\alpha$  radiation and  $\theta$  is the angle obtained from the  $2\theta$  value corresponding to the (101) peak attributed to the anatase  $\text{TiO}_2$ . According to Scherrer's equation, the calculated average crystalline size was found to be  $\approx 11$  nm.

The UV-vis diffuse reflectance spectra of synthesized  $\text{TiO}_2$  nanoparticles in the range of 200-800 nm are shown in **Figure (1b)**, assuming that  $\text{TiO}_2$  has an indirect optical transition



(Sakthivel, Janczarek, and Kisch 2004), the calculated band gap energy for synthesized TiO<sub>2</sub> is 3.223 eV.

The surface morphology and texture of catalyst are one of the important parameters might influence the photocatalytic efficiency, the annealed TiO<sub>2</sub> nanoparticles were investigated by FE-SEM image as shown in **Figure (1c)**. The SEM image depicts that the particles are in the form of aggregates and the surface of the annealed TiO<sub>2</sub> is irregular with the size range of 12–20 nm or even smaller.

**Figure (1d)** shows typical atomic force microscopy AFM images of TiO<sub>2</sub> film. It can be seen that this film is quite uniform. The particle-size distributions of TiO<sub>2</sub> film in AFM image was about 55–82 nm, much greater than the crystallite sizes studied from the XRD. The aggregation of the primary crystallites caused to the increase in the crystallite sizes of TiO<sub>2</sub> particles measured in AFM results.

### UV–visible Spectra of GRL Photocatalytic Reaction

**Figure 2** displays the changes in the UV–vis adsorption spectra of 15 mg L<sup>-1</sup> GRL neutral solution exposed to the UVA for different time in the presence of 2 g L<sup>-1</sup> TiO<sub>2</sub>.

The spectrum of GRL shows that the intensity of the peaks at 609 nm ( $\lambda$  max) decreases gradually during the UVA irradiation, resulting in decolorization of the solutions. The diminished absorption intensity of the  $\lambda$ max also expresses the loss of conjugation, e.g., especially the cleavage nears the azo bond from the  $-N = N$  double bond as the most active site for the oxidation attack (Sun et al. 2002). The nearly perfect disappearance of the band at 609 nm reveals that GRL is eliminated after about 60 min.

This is accompanied by a parallel decrease of the intensity of the peak in the UV region, 296 nm, attributed to the benzothiazol ring. No new absorption peaks appeared in either visible or UV regions.

Control experiments (Figure not shown) proved that the decolorization of GRL was not feasible in the absence of either UVA light or photocatalyst TiO<sub>2</sub>. On the other hand, the use of UVA light and photocatalyst resulted in significant GRL decolorization efficiency.

## **Factors Affecting on Photocatalytic Degradation of GRL Dye**

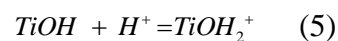
### **Effect of Catalyst Loading**

A set of experiments was carried out to attain the optimum catalyst loading by varying the amount of TiO<sub>2</sub> catalyst from 0.25 to 4 g L<sup>-1</sup> (**Figure 3**). Results show the apparent rate constant and relative photonic efficiency of GRL degradation, increased as TiO<sub>2</sub> content increased to 3 g L<sup>-1</sup> from 0.25 g L<sup>-1</sup>. However, further adding TiO<sub>2</sub> content in the reacting system resulted in reduced photocatalytic degradation of GRL dye.

This attributed to that the increase in the amount of TiO<sub>2</sub> nanoparticles caused to increase the number of active sites on the photocatalyst surface, which in turn increase the number of superoxide and hydroxyl radicals. This could be explained by the fact that the collision frequency between oxidants and maxilon blue GRL would affected by an increase in TiO<sub>2</sub> dosage (Miao et al. 2014). Furthermore, the apparent rate constant and relative photonic efficiency reduced due to the retardation of the light by the suspension when the concentration of the catalyst increases above the optimum value (Muruganandham and Swaminathan 2006).

### **Influence of pH**

The performance of solution pH effects is a very difficult function on the efficiency of dye photocatalytic degradation process because of its multiple roles (Akpan and Hameed 2009) such as the related to the ionization state of the surface according to the following reactions,



Also the role hydroxyl radicals can be formed by the reaction between hydroxide ions and positive holes. In addition, it should also be cleared that under acidic condition the surface area available for dye adsorption and photon absorption would be reduced because  $\text{TiO}_2$  particles tend to agglomerate (Fox and Dulay 1993). The apparent rate constant and relative photonic efficiency of GRL in the presence of  $\text{TiO}_2$  nanoparticles was studied at different pH values ranging from 3 to 11. Prior to  $\text{TiO}_2$  addition, the photostability of GRL at different pH values was tested in the absence of  $\text{TiO}_2$ . GRL dye becomes completely dissociated at high pH values due to the complete ionization of hydroxyl and sulfonate groups.

The results show that  $\text{TiO}_2$  nanoparticles exhibit better the apparent rate constant and relative photonic efficiency at pH 5 (**Figure 4**), since pH of solutions dependent to the surface-charge-properties of the semiconductors. The highly photostability of the undissociated species under acidic conditions, at  $\text{pH} < 5$ , caused to decrease the apparent rate constant and relative photonic efficiency.

### **Effect of Initial Dye Concentration**

The effect of various initial dye concentrations at different interval times on the degradation of GRL on  $\text{TiO}_2$  surface has been investigated. Since the generation of reactive oxygen species ROSs has remained constant, the probability of dye molecule to react with

reactive species decreases. The photocatalytic degradation efficiency decreases at higher initial dye concentrations, while at low concentration the increasing photon absorption by the catalyst thereby reverse effect is observed.

However, the formation of  $\text{OH}^\cdot$ ,  $\text{O}_2^\cdot$  or  $\text{h}^+$  on the catalyst surface remains constant for a given catalyst amount, light intensity, and irradiation time. Therefore, at higher concentrations, the available  $\text{OH}^\cdot$  radicals are inapplicable for pollutant degradation. Consequently, the rate of photocatalytic degradation increased when the pollutant concentration increases (Bahnemann, Muneer, and Haque 2007).

It is well known that the rate of photocatalytic degradation strongly depends on both the concentration of organic compound used as the test molecule (GRL) and on the intensity of the incident light (Tschirch, Dillert, and Bahnemann 2008). This expression is usually explained by the empirical kinetic model given in equation (7), *i.e.*, called Langmuir – Hinshelwood rate law (L-H): (Kormann, Bahnemann, and Hoffmann 1991; Hoffmann et al. 1995)

$$r_{\text{GRL}} = \frac{k_r \cdot K_{\text{ads}} \cdot [\text{GRL}]_{\text{ads}}}{1 + K_{\text{ads}} \cdot [\text{GRL}]_0} \cdot I_{\text{hv}}^\beta \quad (7)$$

$$r_{\text{GRL}} = k_{\text{ap}} \cdot [\text{GRL}] \quad (8)$$

$$k_{\text{ap}} = k_r \cdot \theta \cdot I_{\text{hv}}^\beta \quad (9)$$

$$\theta = \frac{K_{\text{ads}} \cdot [\text{GRL}]_{\text{ads}}}{1 + K_{\text{ads}} \cdot [\text{GRL}]_{\text{ads}}} \quad (10)$$

Where  $k_r$  a constant of different intermediate rates steps,  $I_{\text{hv}}$  is an incident light intensity of photocatalytic degradation,  $\beta$  is empirical constant,  $\theta$  is the fraction of the surface covered by the reactant, and the  $K_{\text{ads}}$  is the adsorption equilibrium constant for GRL.

The applicability of L–H equation for degradation has been confirmed by the nonlinear plot (correlation coefficient of 0.944), obtained for rate of photodegradation (R) vs. initial dye concentration **Figure 5**. This indicates that the degradation of GRL occurred mainly on the surface of TiO<sub>2</sub>.

### Effect of Light Intensity

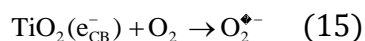
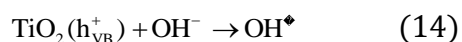
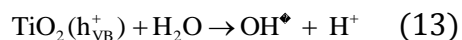
The extent of light absorption by the semiconductor catalyst at a given wavelength was determined by light intensity. The rate of initiation of photocatalysis, and electron–hole formation in the photochemical reaction is strongly dependent on the light intensity (Cassano and Alfano 2000).

**Figure 6** shows plots of the apparent rate constant as well as the relative photonic efficiency as a function of the applied light intensity, **Figure 6** shown a non-linear relation between the apparent rate constant and the employed light intensity was observed, while the relative photonic efficiency would be independent light intensity at high light intensity more than 25 mW cm<sup>-2</sup>. Because at higher light intensity the relative photonic efficiency will decrease, this is attributed to the primary initiator of oxidation of electron-donating substrates and the surface-bound hydroxyl radical would be the principal hole trap when the intensity is increased by about 25 mW cm<sup>-2</sup> (Garcia and Takashima 2003).

### Role of Reactive Oxygen Species (ROSs)

In order to distinguish the contribution of the surface reaction with OH<sup>·</sup>, O<sub>2</sub><sup>-·</sup> or h<sup>+</sup> species, different reactive oxygen species were employed to check their effects on the relative photonic efficiencies of GRL dye.

The reaction pathway of GRL degradation through generation of radicals from photogenerated electron-hole pairs ( $e_{CB}^-$ ,  $h_{VB}^+$ ) is shown as follows (Subramonian and Wu 2014):



It is well known that two main species have the major contributions: hydroxyl radicals and electrons and holes ( $e_{CB}^-$ ,  $h_{VB}^+$ ) affected on the photocatalytic degradation process (Saien and Soleymania 2007). The recombination lifetime of the photo-generated electrons and holes and the interfacial electron-transfer rate were used to determine the overall quantum efficiency of photocatalysis.

To strengthen the quantum efficiency, the most general way is to try to retard the recombination of photo-generated holes and electrons. Therefore, filling the valence band holes by the electrons of some kind of reductant may confirm the photocatalytic efficiency.

In the present study, several scavengers were used, such as EDTA was adopted as the scavengers for  $h^+$  (Lv, Zhu, and Zhu 2013), isopropanol for  $\text{OH}^\bullet$  (Martin, Lee, and Hoffmann 1995), N-phenyl aniline for  $\text{O}_2^{\bullet-}$  (Zhang et al. 2014) and potassium

iodide (KI) for both  $h^+$  and  $OH^\cdot$ . (Zhang et al. 2008; Van Doorslaer et al. 2012) As can be seen from **Figure 7**, the photocatalytic degradation efficiency of GRL is 62.93% without scavengers after irradiation for 60 min.

When isopropanol was added, the degradation efficiency changed and reduced to 18.9%, indicating that  $OH^\cdot$  can be important in the photocatalytic process, also the presence of N-phenyl aniline remarkably slightly reduces the photocatalytic activity of GRL under the same condition to 38.56%, which suggests that  $O_2^{\cdot-}$  is the secondary active species in the reaction. On the other hand, the presence of N-phenyl aniline or  $Na_2EDTA$  remarkably slightly reduces the photocatalytic activity of GRL under the same condition to 38.56%, 33.43% respectively which suggests that  $O_2^{\cdot-}$  and  $h^+$  they are not main active species in the reaction.

## CONCLUSION

In summary, synthesized  $TiO_2$  nanoparticles were used as a prospect efficient photocatalyst for the studying of relative photonic efficiency of maxilon blue dye (GRL). The investigation of photocatalytic ability of synthesized  $TiO_2$  nanoparticles showed that the catalyst activity was influenced by various parameters such as catalyst loading, light intensity, initial solution concentration, initial pH of solution, In addition to the type and amount of reactive oxygen species on the GRL dye degradation. The most favorable results for the photocatalytic degradation of GRL dye were observed at pH 5 at a catalyst loading of  $3\text{ g L}^{-1}$ . The increase of initial dye concentration decreases the degradation rate. The applicability of Langmuir–Hinshelwood kinetic model reveals that the photocatalytic degradation of GRL dye occurs mainly on the surface of the photocatalyst. The further study of the contribution of the ROSs

indicates that both OH<sup>·</sup> and particular h<sup>+</sup> together are responsible for the major photocatalytic degradation of GRL, the other ROSs play an insular role during this process.

## Acknowledgment

The authors gratefully acknowledge the assistance provided by Babylon University, College of science for Women/Chemistry Department.

## References

- Akpan, U. G., and B. H. Hameed. 2009. Parameters affecting the photocatalytic degradation of dyes using TiO<sub>2</sub>-based photocatalysts: A review. *Journal of Hazardous Materials* 170 (2-3):520-529.
- Aljeboree, A. M., A. F. Alkaim, and A. H. Al-Dujaili. 2015. Adsorption isotherm, kinetic modeling and thermodynamics of crystal violet dye on coconut husk-based activated carbon. *Desalination and Water Treatment* 53 (13):3656-67. doi:10.1080/19443994.2013.877854
- Aljebori, A. M., and A. N. Alshirifi. 2012. Effect of Different parameters on the adsorption of textile dye maxilon blue GRL from aqueous solution by using white marble. *Asian Journal of Chemistry* 24 (12):5813-16.
- Alkaim, A. F., R. Dillert, and D. W. Bahnemann. 2015. Effect of polar and movable (OH or NH<sub>2</sub> groups) on the photocatalytic H<sub>2</sub> production of alkyl-alkanolamine: A comparative study. *Environmental Technology* 36 (17):2190-97. doi:10.1080/09593330.2015.1024757
- Alkaim, A. F., and F. H. Hussein. 2012. Photocatalytic degradation of EDTA by using TiO<sub>2</sub> suspension. *International Journal of Chemical Sciences* 10 (1):586-98.
- Alkaim, A. F., T. A. Kandiel, F. H. Hussein, R. Dillert, and D. W. Bahnemann. 2013. Solvent-free hydrothermal synthesis of anatase TiO<sub>2</sub> nanoparticles with enhanced photocatalytic hydrogen production activity. *Applied Catalysis A: General* 466:32-37. doi:10.1016/j.apcata.2013.06.033
- Bahnemann, W., M. Muneer, and M. M. Haque. 2007. Titanium dioxide-mediated photocatalysed degradation of few selected organic pollutants in aqueous suspensions. *Catalysis Today* 124 (3-4):133-48. doi:10.1016/j.cattod.2007.03.031
- Bayar, S., R. BoncukcuoÄŸlu, A. E. Yilmaz, and B. A. Fil. 2014. Pre-treatment of Pistachio Processing Industry Wastewaters (PPIW) by electrocoagulation using Al plate electrode. *Separation Science and Technology* 49 (7):1008-18. doi:10.1080/01496395.2013.878847
- Cassano, A. E., and O. M. Alfano. 2000. Reaction engineering of suspended solid heterogeneous photocatalytic reactors. *Catalysis Today* 58 (2-3):167-97. doi:10.1016/s0920-5861(00)00251-0
- Chen, C.-Y. 2009. Photocatalytic degradation of Azo dye reactive orange 16 by TiO<sub>2</sub>. *Water, Air, and Soil Pollution* 202 (1-4):335-42. doi:10.1007/s11270-009-9980-4



- Da Dalt, S., A. K. Alves, F. A. Berutti, and C. P. Bergmann. 2015. Designing of TiO<sub>2</sub>/MWCNT nanocomposites for photocatalytic degradation of organic dye. *Particulate Science and Technology* 33 (3):308–13. doi:10.1080/02726351.2014.970308
- El-Mekkawi, D., and H. R. Galal. 2013. Removal of a synthetic dye “Direct Fast Blue B2RL” via adsorption and photocatalytic degradation using low cost rutile and Degussa P25 titanium dioxide. *Journal of Hydro-environment Research* 7 (3):219–26. doi:10.1016/j.jher.2013.02.003
- Fil, B. A. 2015. Isotherm, kinetic, and thermodynamic studies on the adsorption behavior of malachite green dye onto montmorillonite clay. *Particulate Science and Technology: An International Journal* 1–9. doi:10.1080/02726351.2015.1052122
- Fil, B. A., R. Boncukcuoğlu, A. E. Yilmaz, and S. Bayar. 2014. Electro-oxidation of pistachio processing industry wastewater using graphite anode. *Clean – Soil, Air, Water* 42 (9):1232–38. doi:10.1002/clen.201300560
- Fox, M. A., and M. Dulay. 1993. Heterogeneous photocatalysis. *Chemical Reviews* 93 (1):341–57.
- Garcia, J. C., and K. Takashima. 2003. Photocatalytic degradation of imazaquin in an aqueous suspension of titanium dioxide. *Journal of Photochemistry and Photobiology A: Chemistry* 155 (1–3):215–22. doi:10.1016/s1010-6030(02)00370-2
- Gaya, U. I., and A. H. Abdullah. 2008. Heterogeneous photocatalytic degradation of organic contaminants over titanium dioxide: A review of fundamentals, progress and problems. *Journal of Photochemistry and Photobiology C: Photochemistry Reviews* 9 (1):1–12. doi:10.1016/j.jphotochemrev.2007.12.003
- Gnanaprakasam, A., V. M. Sivakumar, P. L. Sivayogavalli, and M. Thirumarimurugan. 2015. Characterization of TiO<sub>2</sub> and ZnO nanoparticles and their applications in photocatalytic degradation of azodyes. *Ecotoxicology and Environmental Safety* 121:121–25. doi:10.1016/j.ecoenv.2015.04.043
- Hoffmann, M. R., S. T. Martin, W. Choi, and D. W. Bahnemann. 1995. Environmental applications of semiconductor photocatalysis. *Chemical Reviews* 95 (1):69–96. doi:10.1021/cr00033a004
- Islam, S., A. S. Kurny, and F. Gulshan. 2015. Degradation of commercial dyes using Mill scale by photo-fenton. *Environmental Processes* 2 (1):215-224. doi:10.1007/s40710-014-0055-1
- Kandiel, T. A., L. Robben, A. Alkaim, and D. Bahnemann. 2013. Brookite versus anatase TiO<sub>2</sub> photocatalysts: Phase transformations and photocatalytic activities. *Photochemical & Photobiological Sciences* 12:602–09. doi:10.1039/c2pp25217a
- Kansal, S. K., P. Kundu, S. Sood, R. Lamba, A. Umar, and S. K. Mehta. 2014. Photocatalytic degradation of the antibiotic levofloxacin using highly crystalline TiO<sub>2</sub> nanoparticles. *New Journal of Chemistry* 38 (7):3220–26. doi:10.1039/c3nj01619f
- Kormann, C., D. W. Bahnemann, and M. R. Hoffmann. 1991. Photolysis of chloroform and other organic molecules in aqueous titanium dioxide suspensions. *Environmental Science and Technology* 25 (3):494–500. doi:10.1021/es00015a018
- Kul, S., R. Boncukcuoğlu, A. E. Yilmaz, and B. A. Fil. 2015. Treatment of olive mill wastewater with electro-oxidation method. *Journal of the Electrochemical Society* 162 (8):G41–G47. doi:10.1149/2.0451508jes

- Lv, Y., Y. Zhu, and Y. Zhu. 2013. Enhanced photocatalytic performance for the BiPO<sub>4</sub>-x Nanorod induced by surface oxygen vacancy. *Journal of Physical Chemistry C* 117 (36):18520–28. doi:10.1021/jp405596e
- Martin, S. T., A. T. Lee, and M. R. Hoffmann. 1995. Chemical mechanism of inorganic oxidants in the TiO<sub>2</sub>/UV process: Increased rates of degradation of chlorinated hydrocarbons. *Environmental Science & Technology* 29 (10):2567–73. doi:10.1021/es00010a017
- Miao, J., Z. Jia, H. B. Lu, D. Habibi, and L. Zhang. 2014. Heterogeneous photocatalytic degradation of mordant black 11 with ZnO nanoparticles under UV-Vis light. *Journal of the Taiwan Institute of Chemical Engineers* 45:1636–41. doi:10.1016/j.jtice.2013.11.007
- Muruganandham, M., and M. Swaminathan. 2006. TiO<sub>2</sub>-UV photocatalytic oxidation of reactive Yellow 14: Effect of operational parameters. *Journal of Hazardous Materials* 135 (1–3):78–86. doi:10.1016/j.jhazmat.2005.11.022
- Pitchaimuthu, S., S. Rajalakshmi, N. Kannan, and P. Velusamy. 2014. Enhanced photocatalytic activity of titanium dioxide by β-cyclodextrin in decoloration of acid Yellow 99 dye. *Desalination and Water Treatment* 52 (16–18):3392–402. doi:10.1080/19443994.2013.799049
- Saien, J., and A. R. Soleymania. 2007. Degradation and mineralization of Direct Blue 71 in a circulating upflow reactor by UV/TiO<sub>2</sub> process and employing a new method in kinetic study. *Journal of Hazardous Materials* 144 (1–2):506–12. doi:10.1016/j.jhazmat.2006.10.065
- Sakthivel, S., M. Janczarek, and H. Kisch. 2004. Visible light activity and photoelectrochemical properties of nitrogen-doped TiO<sub>2</sub>. *Journal of Physical Chemistry: B* 108 (50):19384–87. doi:10.1021/jp046857q
- Simin, J.-D. 2014. Structural and photocatalytic activity of mesoporous N-Doped TiO<sub>2</sub> with band-to-band visible light absorption ability. *Particulate Science and Technology* 32 (5):506–11. doi:10.1080/02726351.2014.920443
- Sobana, N., B. Krishnakumar, and M. Swaminathan. 2013. Synergism and effect of operational parameters on solar photocatalytic degradation of an azo dye (Direct Yellow 4) using activated carbon-loaded zinc oxide. *Materials Science in Semiconductor Processing* 16 (3):1046–51. doi:10.1016/j.mssp.2013.01.002
- Subramonian, W., and T. Wu. 2014. Effect of enhancers and inhibitors on photocatalytic sunlight treatment of methylene blue. *Water, Air, & Soil Pollution* 225 (4):1–15. doi:10.1007/s11270-014-1922-0
- Sun, J., X. Wang, J. Sun, R. Sun, S. Sun, and L. Qiao. 2006. Photocatalytic degradation and kinetics of Orange G using nano-sized Sn(IV)/TiO<sub>2</sub>/AC photocatalyst. *Journal of Molecular Catalysis A: Chemical* 260 (1–2):241–46. doi:10.1016/j.molcata.2006.07.033
- Sun, Z., Y. Chen, Q. Ke, Y. Yang, and J. Yuan. 2002. Photocatalytic degradation of a cationic azo dye by TiO<sub>2</sub>/bentonite nanocomposite. *Journal of Photochemistry and Photobiology A: Chemistry* 149 (1–3):169–74. doi:10.1016/s1010-6030(01)00649-9
- Tang, W. Z., and H. An. 1995. UV/TiO<sub>2</sub> photocatalytic oxidation of commercial dyes in aqueous solutions. *Chemosphere* 31 (9):4157–70. doi:10.1016/0045-6535(95)80015-d
- Thiruvengkatachari, R., S. Vigneswaran, and I. S. Moon. 2008. A review on UV/TiO<sub>2</sub> photocatalytic oxidation process. *Korean Journal of Chemical Engineering* 25 (1):64–72. doi:10.1007/s11814-008-0011-8

- Tschirch, J., R. Dillert, and D. W. Bahnemann. 2008. Photocatalytic degradation of Methylene blue on fixed powder layers: Which limitations are to be considered? *Journal of Advanced Oxidation Technologies* 11 (2):193–98.
- Van Doorslaer, X., P. M. Heynderickx, K. Demeestere, K. Debevere, H. Van Langenhove, and J. Dewulf. 2012. TiO<sub>2</sub> mediated heterogeneous photocatalytic degradation of moxifloxacin: Operational variables and scavenger study. *Applied Catalysis B: Environmental* 111–12:150–56. doi:10.1016/j.apcatb.2011.09.029
- Vieira, A. P., S. A. Santana, C. B. Bezerra, H. S. Silva, J. P. Chaves, J. P. de-Melo, F. da-Silva, C. Edson, and C. Airoidi. 2009. Kinetics and thermodynamics of textile dye adsorption from aqueous solutions using babassu coconut mesocarp. *Journal of Hazardous Materials* 166 (2–3):1272–78. doi:10.1016/j.jhazmat.2008.12.043
- Wang, J., X. Wang, G. Li, P. Guo, and Z. Luo. 2010. Degradation of EDTA in aqueous solution by using ozonolysis and ozonolysis combined with sonolysis. *Journal of Hazardous Materials* 176 (1–3):333–38. doi:10.1016/j.jhazmat.2009.11.032
- Zhang, X., T. Guo, X. Wang, Y. Wang, C. Fan, and H. Zhang. 2014. Facile composition-controlled preparation and photocatalytic application of BiOCl/Bi<sub>2</sub>O<sub>2</sub>CO<sub>3</sub> nanosheets. *Applied Catalysis B: Environmental* 150–51:486–95. doi:10.1016/j.apcatb.2013.12.054
- Zhang, X., D. D. Sun, G. Li, and Y. Wang. 2008. Investigation of the roles of active oxygen species in photodegradation of azo dye AO<sub>7</sub> in TiO<sub>2</sub> photocatalysis illuminated by microwave electrodeless lamp. *Journal of Photochemistry and Photobiology A: Chemistry* 199 (2–3):311–15. doi:10.1016/j.jphotochem.2008.06.009
- Zhou, H., and D. W. Smith. 2002. Advanced technologies in water and wastewater treatment. *Journal of Environmental Engineering and Science* 1 (4):247–64. doi:10.1139/s02-020

**Figure 1.** Typical (a) XRD pattern, (b) UV-vis Diffuse reflectance (Tauc plot for absorption edge determination in the inset), (c) FE-SEM and (d) AFM images for the calcined TiO<sub>2</sub> nanoparticles.

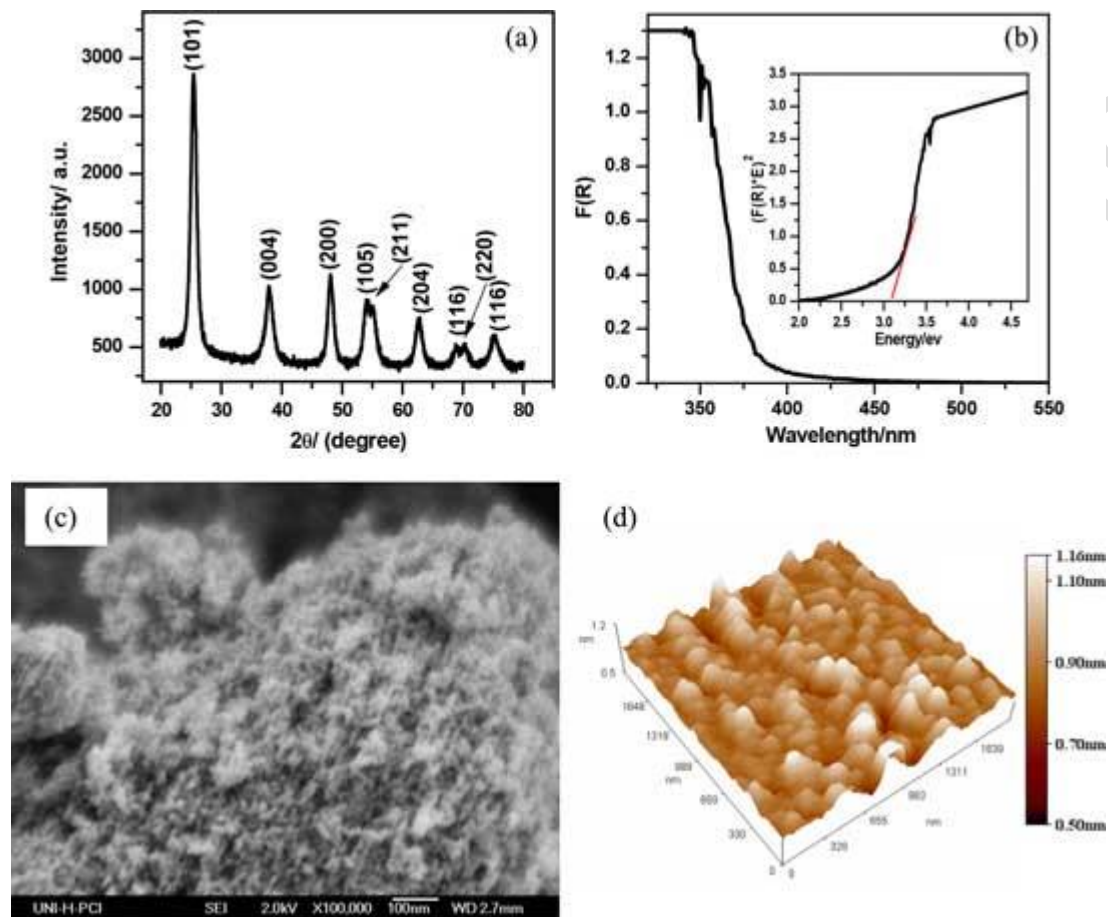


**Figure 2.** UV-vis spectra changes of GRL dye at different times during adsorption and photocatalysis process; Experimental conditions: Catalyst loading  $2 \text{ g L}^{-1}$ ,  $\text{pH} = 6.55$ , GRL conc.  $15 \text{ mg.L}^{-1}$ , light intensity  $33.5 \text{ mW cm}^{-2}$ , irradiation time 60 min.; (inset shows chemical structure of GRL dye).

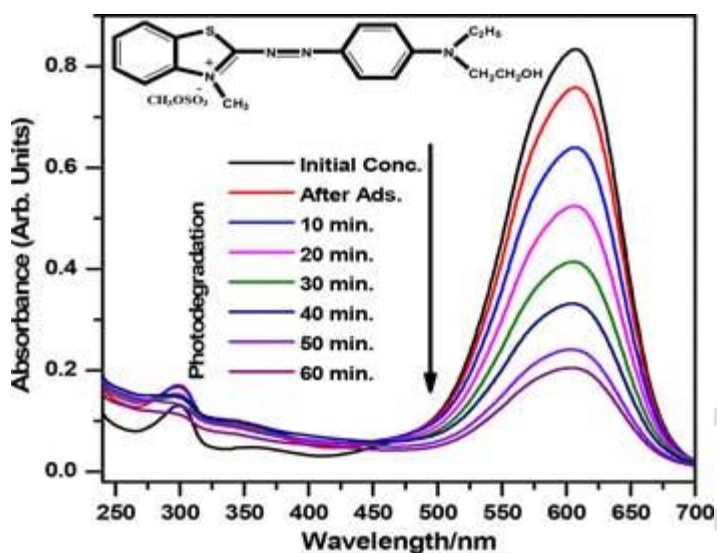


**Figure 3.** Variation of photonic efficiency and apparent rate constant values as a function of amount of catalyst. Experimental conditions: pH = 6.55, GRL conc. 25 mg.L<sup>-1</sup>, light intensity 33.5 mW cm<sup>-2</sup>.

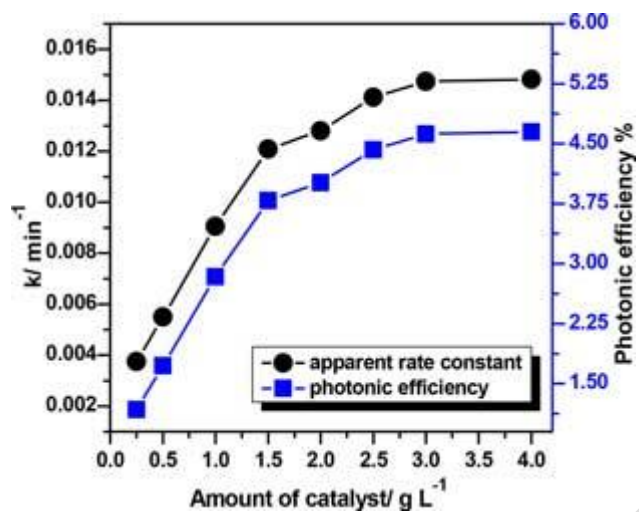


**Figure 4** Variation of photonic efficiency and apparent rate constant values as a function of solution pH. Experimental conditions: Catalyst loading  $3 \text{ g L}^{-1}$ , GRL conc.  $25 \text{ mg.L}^{-1}$ , light intensity  $33.5 \text{ mW cm}^{-2}$ .

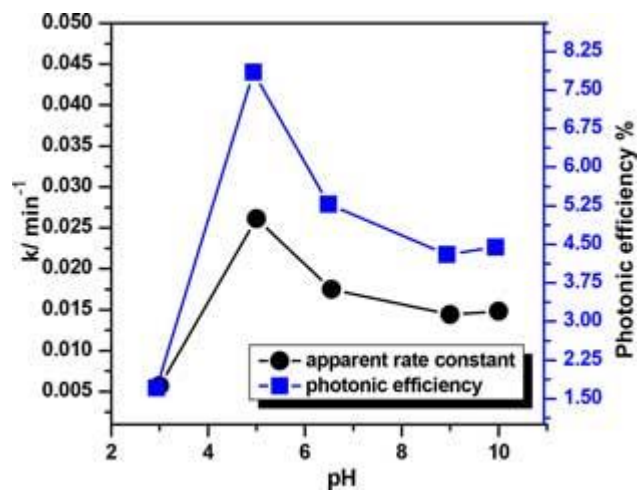


**Figure 5.** Langmuir-Hinshelwood model: (inset variation of PDE % after 75 min). Experimental conditions: Catalyst loading  $2 \text{ g L}^{-1}$ ,  $\text{pH} = 6.55$ , light intensity  $33.5 \text{ mW cm}^{-2}$ .

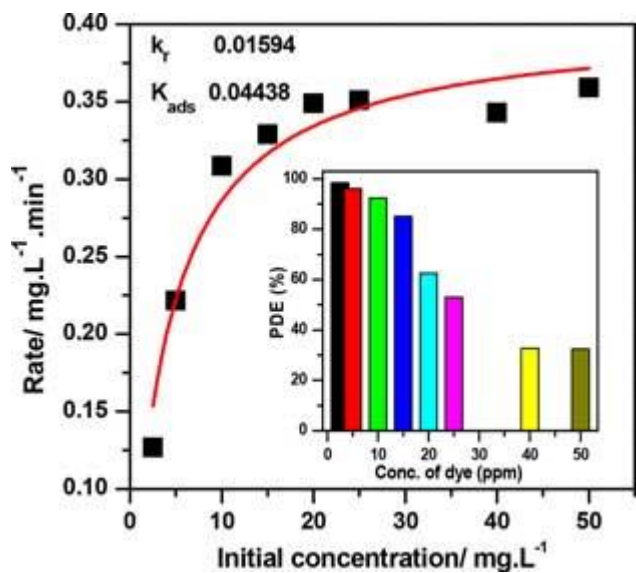
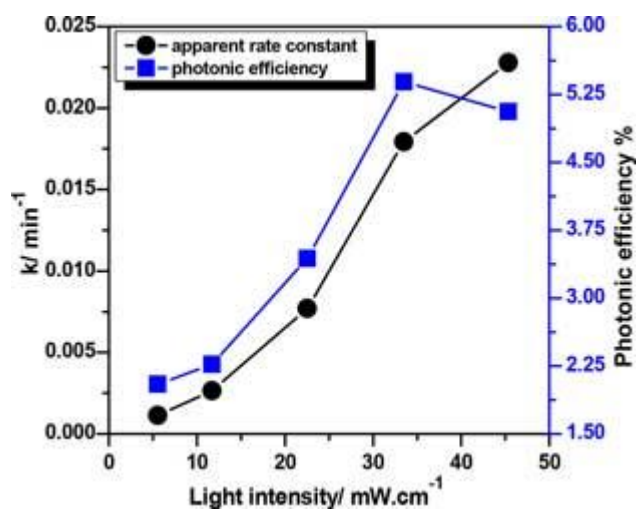




**Figure 6.** Variation of photonic efficiency and apparent rate constant values as a function of light intensity. Experimental conditions: Catalyst loading 3 g L<sup>-1</sup>, pH = 6.55, GRL conc. 25 mg.L<sup>-1</sup>.



Accepted Manuscript

**Figure 7.** Variation of (a) photonic efficiency and (b) photodegradation efficiency as a function of reactive oxygen species (ROs) concentrations. Experimental conditions: Catalyst loading 3 g L<sup>-1</sup>, pH = 6.55, GRL conc. 20 mg.L<sup>-1</sup>, light intensity 33.5 mW cm<sup>-2</sup>.

